Journal of
Manufacturing and Materials Processing

MDPI

Article

Enhancing Mechanical Properties of Hemp and Sisal Fiber-Reinforced Composites Through Alkali and Fungal Treatments for Sustainable Applications

Rahul Kovuru * and Jens Schuster

Department of Applied logistics and Polymers, University of Applied Sciences Kaiserslautern, 66953 Pirmasens, Germany; jens.schuster@hs-kl.de
* Correspondence: rako1001@stud.hs-kl.de

Abstract: The growing demand for sustainable materials has driven interest in natural fiber-reinforced composites as eco-friendly alternatives to synthetic materials. This research investigates the fabrication and mechanical performance of hemp and sisal fiber-reinforced composites, with a focus on improving fiber–matrix bonding through alkali and fungal treatments. Experimental results show that fungal treatment significantly improves tensile and flexural strength, while hardness slightly decreases. Water absorption tests revealed moderate reductions in hydrophilicity compared to untreated samples, although absolute water uptake remains higher than conventional glass/epoxy composites. Microscopy analysis further confirmed enhanced fiber adhesion and structural integrity in treated specimens. These findings suggest that hybrid composites reinforced with hemp and sisal, particularly with fungal treatment, hold promise for low-to-medium load sustainable applications in the automotive interiors, packaging, and construction industries, where moderate mechanical performance and partial biodegradability are acceptable. This research contributes to the advancement of bio-based composite materials while acknowledging current limitations in long-term durability and complete biodegradability.

Keywords: natural fiber composites; alkali treatment; fungal treatment; hemp and sisal fibers; sustainable materials

Academic Editor: Guido Di Bella

Received: 30 April 2025
Revised: 30 May 2025
Accepted: 3 June 2025
Published: 10 June 2025

Citation: Kovuru, R.; Schuster, J. Enhancing Mechanical Properties of Hemp and Sisal Fiber-Reinforced Composites Through Alkali and Fungal Treatments for Sustainable Applications. *J. Manuf. Mater. Process.* **2025**, *9*, 191. https://doi.org/10.3390/jmmp9060191

1. Introduction

Composite materials are engineered substances composed of two or more distinct components, designed to combine desirable properties such as strength, stiffness, and durability that individual materials alone cannot achieve. The matrix, typically made of polymer, metal or ceramic, binds the reinforced fibers or particles, which serve to enhance specific characteristics of the material. In the case of polymer matrix composites (PMCs), organic matrix materials are reinforced with high-strength fibers like carbon, glass, or aramid, significantly improving mechanical and thermal properties. However, the environmental impact of synthetic fibers, particularly after their life cycle ends, has led to growing interest in sustainable alternatives. The growing demand for sustainable materials has driven significant research into natural fiber-reinforced composites as an environmentally friendly alternative to synthetic fibers [1,2]. Balaga et al. [3] focused on the sustainability aspect by demonstrating a successful recycling approach for carbon fibers, allowing them to be reused in high-performance applications. While this helps reduce the embodied energy of carbon fiber components, further gains in sustainability can be made by replacing certain applications with natural fibers such as hemp and sisal.

These natural fibers offer key advantages like biodegradability, low cost, and a much lower environmental footprint. Utilizing natural fibers in composite processing pushes the sustainability boundary even further, making the material choice more environmentally responsible without compromising functionality. These fibers are increasingly being used in various industries, including automotive, construction, and packaging, due to their lightweight and renewable nature [4].

Natural fibers such as hemp and sisal have emerged as competitive reinforcements in composite materials, combining substantial mechanical properties with environmental benefits. As demonstrated by Shahzad [5], hemp fibers exhibit exceptional tensile strength (250–900 MPa) and stiffness (30–60 GPa), making them viable alternatives to synthetic fibers in structural applications. These natural fibers offer a unique combination of high specific modulus, low density (1.4–1.5 g/cm^3), and sustainable attributes, including biodegradability and renewability. Particularly in automotive and aerospace applications, hemp fibers provide an optimal balance between mechanical performance and ecological responsibility, with their specific stiffness.

Complementing hemp fibers, sisal fibers (Agave sisalana) offer distinct advantages as composite reinforcements, particularly where impact resistance and cost efficiency are paramount. With tensile strength (400–700 MPa) and Young's modulus (9–22 GPa), sisal fibers provide exceptional toughness—absorbing up to 50% more energy before fracture compared to hemp fibers at similar loading levels. Their natural cellular structure, featuring elongated fiber bundles with high cellulose content (67–78%), contributes to this enhanced damage tolerance. As documented by Bledzki et al. [6], these properties make sisal fibers ideal for applications requiring repeated impact resistance, such as automotive interior panels, protective packaging, and construction materials.

When hemp and sisal fibers are combined in hybrid composites, their complementary properties can result in a material that benefits from both fiber strengths. Hemp fibers contribute to the stiffness and strength of the composite, while sisal fibers enhance toughness and impact resistance, creating more balanced and efficient composite material. Moreover, hybridization of these fibers can help reduce the overall material costs, as both fibers are relatively low-cost and abundant, making them an attractive choice for large-scale manufacturing [7]. To better understand the suitability of hemp and sisal for composite applications, Table 1 compares their mechanical properties with other natural fibers and conventional synthetic reinforcements.

Table 1. Comparison of mechanical properties of natural and synthetic fibers used in composites.

Fiber Type	Tensile Strength (MPa)	Young's Modulus (GPa)	Density (g/cm^3)
Hemp [6]	250–900	30–60	1.4–1.5
Sisal [7]	400–700	9–22	1.3–1.5
Flax [8,9]	500–1500	50–70	1.4–1.5
Jute [10]	200–800	10–30	1.3–1.5
E-Glass [11]	2000–3500	70–85	2.54
Carbon [12]	4000–6000	230–600	1.75–2.00

Recent advancements have also highlighted the potential of combining natural fibers with polypropylene (PP) matrices for automotive and semi-structural applications. For example, Kumar et al. [13] developed hybrid composites using Himalayan agave fibers (HAFs) and graphene oxide-treated fly ash as reinforcements in a toughened PP matrix. The resulting composites exhibited significant improvements in tensile, flexural, and impact properties compared to neat PP, demonstrating the effectiveness of simultaneous fiber treatment and secondary reinforcement strategies. Such studies reinforce the growing

interest in plant-based fiber composites as sustainable alternatives to conventional materials in lightweight engineering applications.

One challenge in using natural fibers in composites is their inherent hydrophilicity, meaning that they naturally attract moisture. This property can lead to poor adhesion between the fibers and polymer matrices. Poor fiber matrix adhesion often results in suboptimal mechanical properties, such as reduced strength and durability of the composite material [14,15]. To overcome this issue, surface modifications including chemical treatments such as alkali treatment, silane treatment, and acetylation or the use of coupling agents are often employed to improve the fiber–matrix interaction, enhancing the overall performance of the composite materials. Despite this challenge, the growing interest in natural fiber composites continues to drive research into effective solutions for improving their properties and broadening their applications in various industries [16,17]. Recent work by Marquard et al. [18] on flax fiber–polypropylene composites under accelerated environmental aging conditions highlights the importance of understanding how ultraviolet (UV) exposure, temperature, and humidity affect the long-term durability of natural fiber thermoplastics. Their study demonstrates that moisture-induced swelling and UV-driven crystallinity changes in polypropylene can significantly influence mechanical and thermal properties over time—reinforcing the need for aging protocols in biocomposite design.

Sreekala et al. [19] pioneered the understanding of alkali treatment effects through their seminal 1997 study of oil palm fibers, establishing a fundamental framework now applied to hemp and sisal fibers. Their work revealed that sodium hydroxide (NaOH) solutions (optimal 5–8% concentration) selectively degrade amorphous components through three transformative mechanisms: First, lignin and hemicellulose dissolution create micro-pitted surfaces (20–50 nm roughness increase) that enhance mechanical interlocking. Second, wax removal exposes reactive hydroxyl groups, increasing surface energy by 30–40% and improving polymer wettability. Third, the preferential etching of disordered cellulose regions boosts crystallinity from 65% to 78–82%, as confirmed by their XRD analyses. The authors quantified how these changes collectively improve fiber performance—tensile strength increased 25 $\pm$ 3%, while moisture absorption decreased from 12% to 7 $\pm$ 0.5%—making their methodology the gold standard for natural fiber pre-treatment.

Gulati et al. [20] introduced fungal treatment as an eco-friendly alternative for modifying natural fibers in their study. Their innovative approach uses living fungi (mycelium) to naturally clean and prepare fiber surfaces. Here is how it works: as the fungi grow, they produce enzymes that gently break down lignin and hemicellulose—the same components removed by harsh chemicals in traditional treatments. This biological process offers three key benefits: (1) it creates a rougher fiber surface for better mechanical bonding, (2) leaves behind natural fungal fibers that help bridge the gap between plant fibers and plastics, and (3) avoids toxic chemicals completely. The authors demonstrated that this method could improve composite strength by 15–20% while being completely biodegradable. However, important questions remain—especially for mixed fiber composites like hemp–sisal blends. We still need more research to understand how fungal treatment affects water resistance, long-term durability, and performance with different fiber combinations. Their pioneering work established the potential, but current studies are now working to optimize these biological treatments for real-world applications.

Sałasińska et al. [21] demonstrated how fiber content and processing conditions critically impact natural fiber composites. Their study revealed three key findings: First, fiber loading between 30 and 40% typically gives the best balance—enough fibers to provide strength but not so many that they clump together. Second, processing temperature matters greatly—keeping epoxy below 120 °C prevents fiber damage while ensuring proper curing. Third, pressure during molding must be carefully controlled; too little causes voids, while

too much can break delicate natural fibers. The researchers tested these factors using hemp fibers in epoxy, showing that optimized conditions could improve strength by 25% compared to poorly made samples. However, they caution that each fiber type behaves differently—what works for hemp might not work for sisal or flax. Their work proves that we cannot just focus on fiber treatment alone; the entire manufacturing process needs equal attention to obtain high-quality composites.

While natural fiber composites cannot match the absolute performance of synthetic counterparts, their sustainability merits justify developing incremental improvements. As demonstrated by Shahzad [5], even modest 10–20% enhancements in natural fiber composite properties can enable their use in semi-structural applications (e.g., automotive interiors, temporary structures) where full biodegradability is prioritized over decades-long durability. This study focuses on optimizing interfacial properties within the inherent constraints of plant fiber/epoxy systems, recognizing that (a) fibers constitute only 30–40% of the composite and (b) moisture resistance will always trail glass fiber composites. Our approach targets applications where a 3–5-year service life is acceptable and where 30–50% weight savings offset the 15–20% cost premium versus conventional materials.

The following sections provide a comprehensive overview of this research: Section 2 outlines the materials used and the experimental methodology, including details of alkali and fungal treatments as well as composite fabrication techniques. Section 3 presents the mechanical, physical, and microstructural characterization results. Section 4 discusses the significance of these findings in the context of natural fiber composites. Section 5 concludes with key outcomes of this study, and Section 6 proposes future research directions aimed at enhancing the sustainability and performance of bio-based composites.

2. Materials and Methods

2.1. Materials

The hemp fiber used in this study was sourced from Apple Oak Fiber Works in China. The sisal fiber used in this study was purchased from eBay and is derived from the Agave sisalana plant in Kenya, East Africa. Mycelium spores were ordered from Etsy. A 10 wt.% solution of NaOH was supplied by Carl Roth GmbH, Karlsruhe, Germany. IN2 epoxy resin was purchased from Easy Composites. Detailed descriptions of the fibers and resin are provided in the tables below. The mechanical properties listed in Tables 2–4 were obtained from the literature sources [5–7,22] and were used as reference values for material selection and composite design.

Table 2. Properties of hemp fiber [5].

Property	Value
Tensile strength	250–900 MPa
Young's modulus	30–60 GPa
Density	1.4–1.5 g/cm^3

Table 3. Properties of sisal fiber [6].

Property	Value
Tensile strength	400–700 MPa
Young's modulus	9–22 GPa
Density	1.3–1.5 g/cm^3

Table 4. Properties of IN2 epoxy [22].

Property	Value
Tensile strength	63.5–73.5 MPa
Young's modulus	2.6–3.8 GPa
Flexural modulus	3.35 GPa
Density	1.5 g/cm^3
Viscosity (at 20 °C)	200–450 mPa.s.

2.2. Alkali Treatment

The alkali treatment was performed using a 4 wt.% sodium hydroxide solution (NaOH), sourced from carlroth.com [23], to enhance fiber–matrix adhesion by removing impurities such as lignin, hemicellulose, and surface oils. The dried hemp and sisal fibers were immersed in NaOH solution for 4 h at room temperature, maintaining a 1:10 fiber-to-liquid ratio by weight to ensure uniform treatment. After the soaking process the fibers were rinsed 2 to 3 times with distilled water to remove the residual NaOH. Finally, the fibers were oven dried at 60 °C for 24 h, to eliminate moisture and remaining impurities, improving their surface roughness and bonding capability with polymer matrix [24,25].

2.3. Fiber Architecture and Layup Design

The composites incorporated a hybrid reinforcement system of plain-woven hemp fabric (areal density: 350 ± 10 g/m^2) and randomly laid chopped sisal fibers (average length: 7 ± 0.5 mm). A controlled five-layer symmetric stacking sequence was implemented: (1) outer woven hemp layer, (2) randomly distributed sisal fibers, (3) central woven hemp layer, (4) second random sisal fiber layer, and (5) outer woven hemp layer. This design achieved critical objectives: first, the bidirectional hemp fabrics provided in-plane stability and tensile strength along warp/weft directions; second, the chopped sisal fibers created a 3D interlaminar network that improved out-of-plane toughness and fungal treatment effectiveness (by increasing surface area for mycelium colonization). Fiber content was precisely regulated according to the experimental design (Table 4), with sisal fibers manually distributed to achieve 85–90% aerial coverage. The architecture balanced the competing demands of mechanical performance (through continuous hemp layers) and treatment accessibility (via discontinuous sisal phases), though this compromise inherently limited maximum theoretical modulus due to fiber misorientation effects.

2.4. Fungal Treatment

The fungal treatment was conducted using mycelium spores to improve both the biodegradability and structural integrity of composite material. The alkali-treated hemp and sisal fibers were first sterilized by autoclaving in the autoclave shown in Figure 1 at 125 °C for 20 min to eliminate any contaminants that could interfere with mycelium growth.

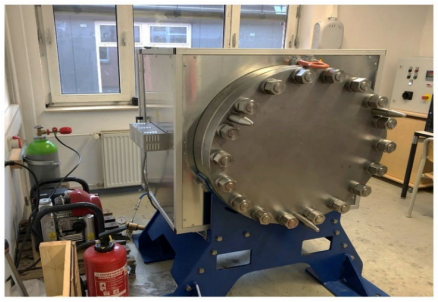

Figure 1. Autoclave.

2.4.1. Substrate Preparation

A suitable substrate as shown in Figure 2 was prepared to support fungal growth, providing both nutrients and structural support. The substrate consisted of a mixture of rice husk, wheat husk, and sawdust, selected for their organic content and porosity, which promotes effective fungal colonization. These materials were dried and finely ground to create a uniform medium. The substrate was then sterilized using an autoclave at 125 °C for 20 min to eliminate unwanted microorganisms [26].

Figure 2. Substrate preparation.

2.4.2. Inoculation and Incubation

After sterilization, the fibers and substrate were inoculated with mycelium spores as indicated in Figure 3 in a controlled, nutrient-rich environment. This step ensured even fungal distribution and efficient colonization. The inoculated mixture as shown in Figure 4 was secured in breathable containers that allowed gas exchange [27]. The incubation conditions were carefully regulated at room temperature (23 °C) with 70–80% relative humidity for 12–15 days, allowing the mycelium to spread and form an interwoven network, effectively binding the fibers together.

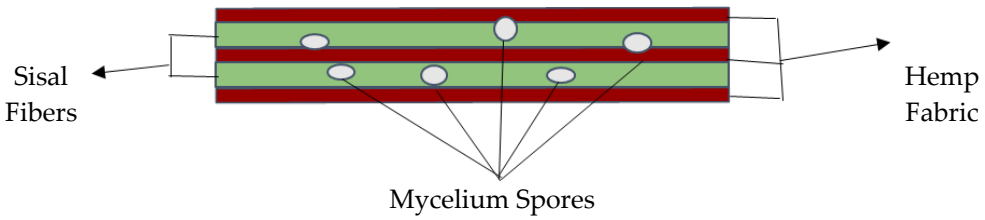

Figure 3. Inoculation.

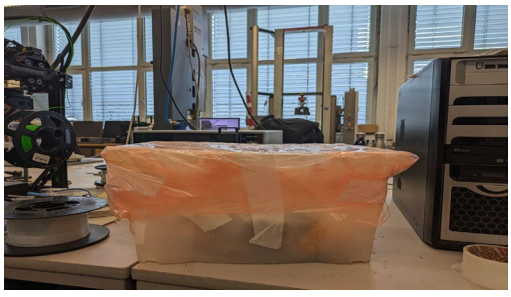

Figure 4. Incubation.

2.4.3. Drying and Final Preparation

Once full colonization was achieved, the fungal-treated fibers were oven-dried at 60 °C for 24 h to halt further growth and reduce moisture content. This step ensured that the composite material was structurally stable and ready for further processing.

2.5. Design of Experiments

The experimental design was developed to evaluate the effects of different variables on the performance of composite material. The Table 5 below outlines the experimental conditions, showing the factors and corresponding treatments used in this study.

Table 5. Design of experiments.

Sample ID	Hemp (wt.-%)	Sisal (wt.-%)	Fiber vol. (ϕ_f)	Epoxy (wt.-%)	Alkali Treatment	Fungal Treatment
S1	15	20	36.2	65	Untreated	Untreated
S2	15	15	30.1	70	Treated	Untreated
S3	15	20	36.2	65	Treated	Untreated
S4	15	15	30.1	70	Treated	Treated
S5	15	20	36.2	65	Treated	Treated
S6	15	25	41.3	60	Treated	Treated

2.6. Sample Preparation

The composite specimens were fabricated using the hand-layup assisted vacuum bagging process, following an initial trial with vacuum-assisted resin transfer molding (VARTM) as illustrated in Figure 5. The VARTM process resulted in excessive void content due to improper resin flow and fiber wetting, necessitating shift to hand-layup assisted vacuum bagging technique to achieve better fiber impregnation and uniform composite structure [28,29].

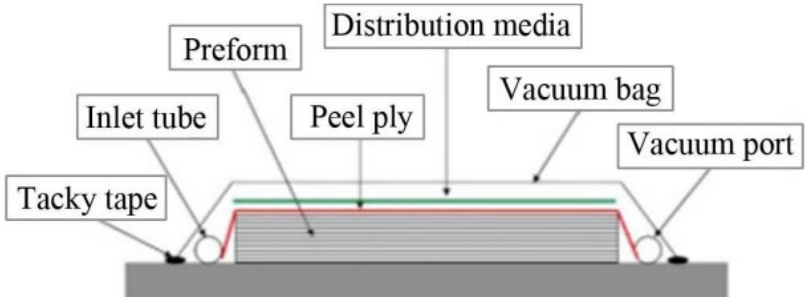

Figure 5. Schematic diagram of hand-layup assisted vacuum bagging process [28].

The fabrication process was adopted from the method reported by Abdurohman [30] and Mujahid [31], applied to both alkali-treated and fungal-treated fibers, as outlined in the experimental design. To ensure proper demolding, a mold release agent (silicon spray) was applied to the mold before placing the fibers. The pre-treated hemp and sisal fibers, as specified in the experiment, were arranged in layers inside the mold according to their designated weight fractions. Epoxy resin, serving as the matrix material, was then applied to the fiber layers using a brush to ensure complete wetting. To remove trapped air and achieve uniform resin distribution, a roller was used with mild pressure, squeezing out excess resin while improving fiber–matrix adhesion.

Once the fiber and resin layup were completed, a peel ply layer was placed on top of the laminate to assist in demolding and provide better surface finish for future processing. A more breathable fabric was also added to facilitate air evacuation and absorb excess resin during vacuum application. The entire assembly was enclosed within a vacuum bag, and its edges were sealed with silicone tape as shown in the Figure 6 to create an airtight environment. A vacuum pump was connected to the setup, applying a uniform pressure of approximately −1 bar to consolidate the composite structure. The vacuum-assisted process

is crucial for minimizing void content, improving fiber/resin interaction, and ensuring consistent laminate thickness.

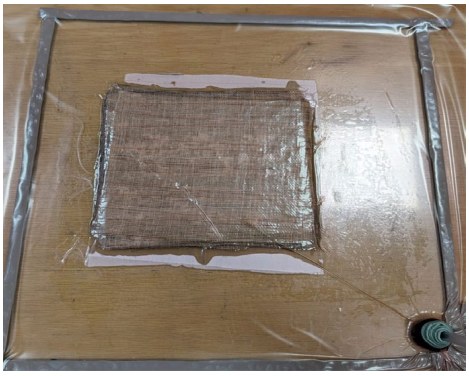

Figure 6. Hand-layup assisted vacuum bagging setup.

The composite specimens were maintained under vacuum for 48 h to allow the resin to fully cure at room temperature. After pre-curing, the samples underwent post-curing in an oven at 40 °C for 6 h to enhance resin cross-linking and improve mechanical integrity of the composite. Once fully cured, the composite sheets were carefully removed from the mold and cut into required dimensions for mechanical testing and characterization.

The volume fraction of the fibers and matrix was determined using the following formula [32]:

$$\phi_f = \frac{\frac{w_{f1}}{\rho_{f1}} + \frac{w_{f2}}{\rho_{f2}}}{\frac{w_{f1}}{\rho_{f1}} + \frac{w_{f2}}{\rho_{f2}} + \frac{w_m}{\rho_m}} \quad (1)$$

where

ϕ_f = fiber volume ratio, w_{f1} = weight of hemp, ρ_{f1} = density of hemp, w_{f2} = weight of sisal, ρ_{f2} = density of sisal, w_m = weight of matrix (epoxy), and ρ_m = density of matrix (epoxy).

Since the fiber and matrix content in the design of experiments was initially provided in weight percentages (wt.%), these values were converted into volume fractions using the above formula to ensure accurate material characterization.

2.7. Test Equipment and Test Parameters

2.7.1. Tensile Test

The tensile properties of the composite samples were evaluated using Zwick universal testing machine, following the DIN EN ISO 527 [33] test standard. The testing procedure was conducted in accordance with the standard, ensuring accurate measurement of material's properties, including tensile strength, Young's modulus, and elongation at break.

For each composition, six standard rectangular specimens were prepared to ensure statistical reliability. The specimen dimensions were 120 mm × 10 mm × 5 mm. The test was conducted with a crosshead speed of 5 mm/min, and Young's modulus was determined within the strain range of 0.05% to 0.25%. The initial grip-to-grip separation was set to 115.00 mm, with a preload of 0.1 N applied before testing to ensure proper specimen alignment. The maximum force capacity of the machine was 10 kN, while the universal testing machine itself had a maximum load of 20 kN.

The TestXpert II software V2 was used to record the force–displacement data and generate stress–strain curves, enabling a detailed analysis of the composite's mechanical performance. The final tensile strength and modulus values were obtained as the average of six test specimens.

2.7.2. Flexural Test

The flexural properties of the composite samples were performed using a Zwick universal testing machine, according to DIN EN ISO 178 [34] for 3-point bending and in alignment with testing procedures. This approach facilitated the accurate measurement of the material's flexural strength, flexural modulus, and elongation at break.

For each formulation, six specimens with dimensions of 80 mm× 10 mm × 4 mm were prepared to ensure statistical reliability. The test was performed under controlled conditions with a preload of 0.1 MPa, a flexure modulus speed of 2 mm/min, and a test speed of 10 mm/min. The span between supports was set according to the standard requirements to maintain consistency.

2.7.3. Impact Test

The impact testing of composites was performed to evaluate their impact resistance by measuring the energy absorbed during fracture. The Charpy impact test was carried out according to DIN EN ISO 179 [35] test standards, using a RAY-Ran advanced universal pendulum from RAY-Ran Test Equipment Ltd., Nuneaton, Warwickshire, England. This device features a dynamic hammer weight of 0.95 kg, an impact energy of 4 joules, and an impact velocity of 2.9 m/s. Six unnotched specimens, each measuring 80 mm × 10 mm × 4 mm, were tested for each composition. The impact energy was applied to the specimens, and the absorbed energy was recorded. To calculate the impact strength (kJ/m^2), the energy absorbed was divided by the specimen's thickness, with the final result being the average of the six tests conducted.

2.7.4. Shore Hardness

Shore D hardness was measured according to the DIN 53,505 [36] standard using a Zwick Durometer, a versatile testing device from ZwickRoell GmbH & Co. KG, Ulm, Germany. The Shore D scale is commonly used to determine the hardness of hard thermoplastics and elastomer materials. The device uses a cone-shaped indenter with a tip that measures hardness values between 30 and 90 Shore D. A force of 50 N was applied to the top of the device, and the indentation depth is recorded on the gauge as a measure of hardness. The measurement was taken after 15–20 s of the indenter tip penetrating the specimen. Each specimen was tested at five different spots, with each spot 15 mm apart from the others to ensure accurate and consistent results.

2.7.5. Water Absorption Test

The water absorption test was conducted to evaluate the amount of water absorbed by the composite material under specified environmental conditions. This test is essential, as excessive water absorption can lead to swelling, dimensional changes, and the degradation of mechanical properties. The experiments were performed in accordance with the ASTM D570-98 [37] standard. The specimens were first dried in the oven at 90 °C for 24 h to eliminate any residual moisture. After cooling, the dry weight (W1) of each specimen was recorded using a digital weighing machine. The specimens were then fully immersed in distilled water at 25 °C for 10 days. Their weight was recorded daily after gently wiping the surface to remove the excess water, allowing for a time-dependent analysis of water absorption.

The percentage of water absorption was calculated each day using the formula:

$$Water\ absorption\ (\%) = \frac{Wet\ weight - Dry\ weight}{Dry\ weight} * 100 \quad (2)$$

By tracking the weight changes over 10 days, this test provided insights into the absorption kinetics, helping to evaluate the long-term moisture resistance of the composite material. The results are valuable in determining its suitability for applications exposed to humid or wet conditions.

2.7.6. Optical Microscopy

Optical microscopy was conducted to examine the microstructural characteristics of the composite samples, focusing on the fiber distribution, porosity, and interfacial bonding. Sample preparation involved embedding the specimens in epoxy resin and its corresponding hardener, which were accurately measured and mixed in a disposable paper cup according to the specified ratio. The mixture was stirred for at least 5 min to ensure uniform blending. The composite specimens were then immersed in the resin–hardener mixture and allowed to cure for 24 h, resulting in hardened structure suitable for microscopy analysis.

After curing, the samples underwent a grinding and polishing process to achieve a smooth and reflective surface, minimizing surface irregularities that could interfere with microscopic observations. The grinding was performed using silicon carbide (SiC) abrasive papers of progressively finer grit sizes, followed by polishing with a fine diamond suspension to obtain a high-quality finish. Once prepared, the samples were examined using an OLYMPUS BX40 light microscope (OLYMPUS, Tokyo, Japan).

3. Results

All mechanical tests were conducted on six specimens per category to ensure statistical reliability. Error bars shown in Figures 7–15 represent ± one standard deviation from the mean. Standard deviations were calculated based on the raw data using equations provided, and results are presented to indicate the variability and reproducibility of the measurements.

$$Mean\ (\overline{x}) = \frac{\{\sum x\}}{n} \tag{3}$$

$$Standard\ Deviation\ (SD) = \sqrt{\frac{\sum (x - \overline{x})^2}{n - 1}} \tag{4}$$

3.1. Mechanical Properties

Figure 7 illustrates the progressive improvement in tensile modulus with treatment. The untreated specimen (S1) exhibited a tensile modulus of 2268 ± 50 MPa, indicating the baseline stiffness of the composite without any fiber treatment. Alkali-treated specimens (S2 and S3) showed improved tensile modulus values, ranging from 2506 ± 45 MPa to 2609 ± 60 MPa, reflecting the positive impact of alkali treatment on fiber–matrix adhesion. The fungal-treated specimens (S4, S5, and S6) further enhanced the tensile modulus, with values reaching 2659 ± 50 MPa to 3227± 80 MPa. This significant increase suggests that fungal treatment not only improves fiber–matrix bonding but also contributes to the overall rigidity of the composite. The highest tensile modulus was observed in specimen S6, which contained 25% sisal fiber and underwent both alkali and fungal treatments, achieving a value of 3227 ± 80 MPa. The results indicate that increasing the fiber content, along with the use of surface treatments, can effectively improve the stiffness of the composite by enabling better stress transfer through the fiber network. In our study, we observed a clear linear increase in the modulus with increasing fiber content, as shown in Figure 7. This trend is consistent with well-established composite theory, which indicates that mechanical performance improves with higher fiber content, since the fibers serve as the primary load-bearing constituents in a composite. Several studies have emphasized that the modulus of a

fibrous composite is strongly influenced by both the fiber content and the fiber orientation. In our current work, all samples were fabricated using randomly oriented mats, and we ensured consistent processing conditions to maintain uniform fiber orientation across the specimens. As a result, orientation effects were assumed to be constant throughout, and the increase in modulus observed can be attributed primarily to the variation in fiber content.

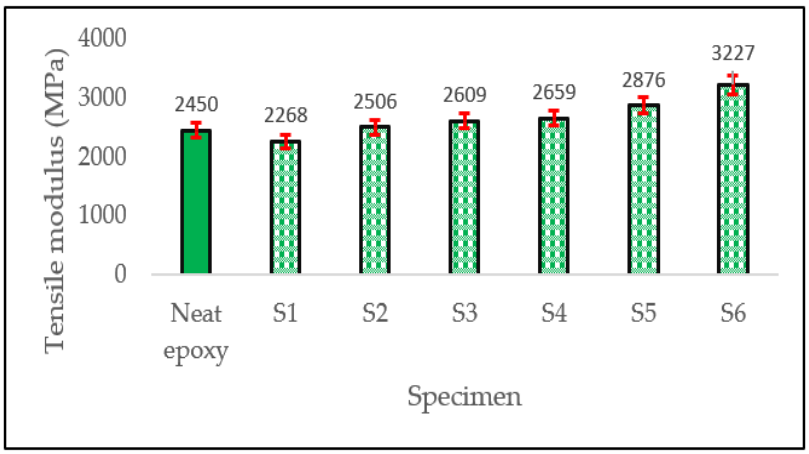

Figure 7. Tensile modulus comparison of different compositions.

Figure 8 provides a graphical representation of the tensile strength values, highlighting the superior performance of fungal-treated specimens. The tensile strength of the untreated specimen (S1) was 32 ± 8 MPa, representing the baseline strength of the composite. Alkali-treated specimens (S2 and S3) showed moderate improvements, with tensile strength values ranging from 39 ± 12 MPa to 41 ± 9 MPa. This increase can be attributed to the removal of surface impurities and better fiber–matrix interaction due to alkali treatment. Fungal-treated specimens (S4, S5, and S6) exhibited the most significant improvement in tensile strength, the values ranging from 44 ± 11 MPa to 55 ± 7 MPa. Specimen S6, with 25% sisal fiber and both treatments, achieved the highest tensile strength of 55 ± 7 MPa, indicating that fungal treatment effectively enhances the load-bearing capacity of the composite. To confirm the statistical significance of variations in tensile strength, a one-way ANOVA was performed across all six specimen types (S1–S6). The analysis yielded an F-value of 5.22 and a p-value of 0.0015, indicating that the observed improvements in tensile strength are statistically significant ($p < 0.05$).

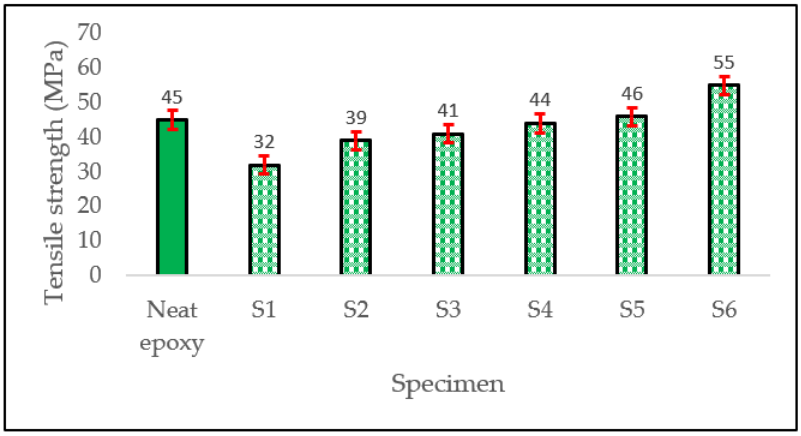

Figure 8. Tensile strength comparison of different compositions.

The representative stress—strain curves (Figure 9) reveal three distinct phases: (1) linear elastic deformation (0–0.5% strain), where fungal-treated samples (S4–S6) exhibit

20–30% steeper slopes, confirming improved fiber–matrix adhesion; (2) non-linear phase (0.5–2.3% strain) dominated by matrix microcracking; and (3) abrupt failure at 2.3% strain, with treated samples retaining higher residual stress (5–10 MPa) due to fiber bridging.

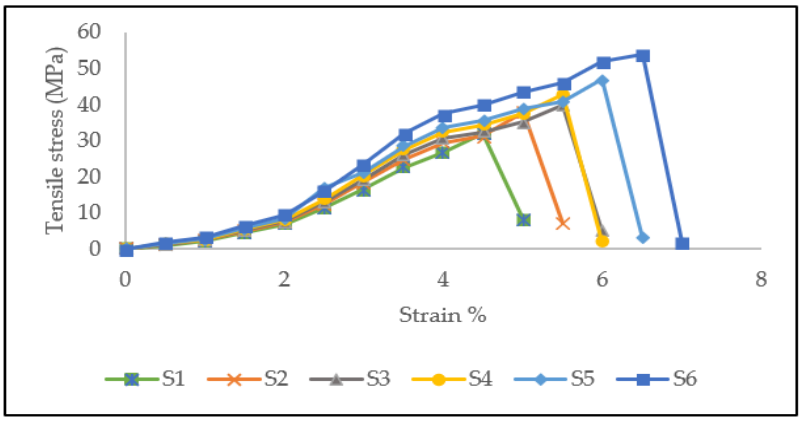

Figure 9. Representative tensile stress–strain curves.

Figure 10 highlights the progressive improvement of flexural modulus with treatment. The flexural modulus of the untreated specimen (S1) was 2150 ± 75 MPa, representing the baseline stiffness of the composite under bending loads. Alkali-treated specimens (S2 and S3) showed moderate improvement with flexural modulus values increasing to 2422 ± 90 MPa and 2465 ± 80 MPa, respectively. This improvement can be attributed to the enhanced fiber–matrix adhesion resulting from the alkali treatment, which removes surface impurities and increases fiber roughness. Fungal-treated specimens (S4, S5, and S6) exhibited the most significant improvement in the flexural modulus, reaching values up to 3300 MPa. Specimen S6, which contained 25% sisal fiber and underwent both alkali and fungal treatments, achieved the highest flexural modulus of 3264 ± 70 MPa, indicating that the fungal treatment not only improves the fiber–matrix bonding but also significantly enhances the composite's rigidity.

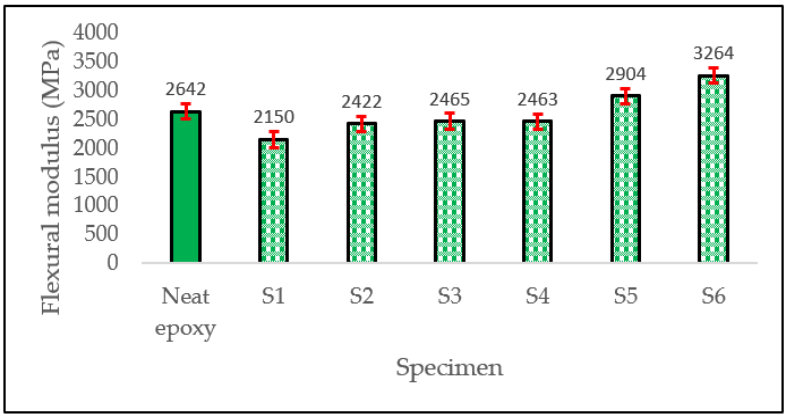

Figure 10. Flexural modulus comparison of different compositions.

Figure 11 provides a graphical representation of the flexural strength values, highlighting the superior performance of fungal-treated specimens. The flexural strength of the untreated specimen (S1) was 36 ± 9 MPa, representing the baseline strength of the composite under bending loads. Alkali-treated specimens (S2 and S3) showed moderate improvements, with flexural strength values ranging from 40 ± 6 MPa to 43 ± 7 MPa. The increase can be attributed to the improved fiber–matrix adhesion resulting from alkali treatment. Fungal-treated specimens (S4, S5, and S6) exhibited the most significant improve-

ment in flexural strength, with values ranging from 48 ± 8 MPa to 55 ± 9 MPa. Specimen S6, with 25% sisal fiber and both treatments, achieved the highest flexural strength of 55 ± 9 MPa, indicating that the fungal treatment effectively enhances the composite's ability to withstand bending stresses. One-way ANOVA was also conducted for flexural strength values across the samples. The results showed a highly significant difference, with an F-value of 9.92 and a p-value < 0.0001, confirming that the fiber treatments led to meaningful differences in flexural performance.

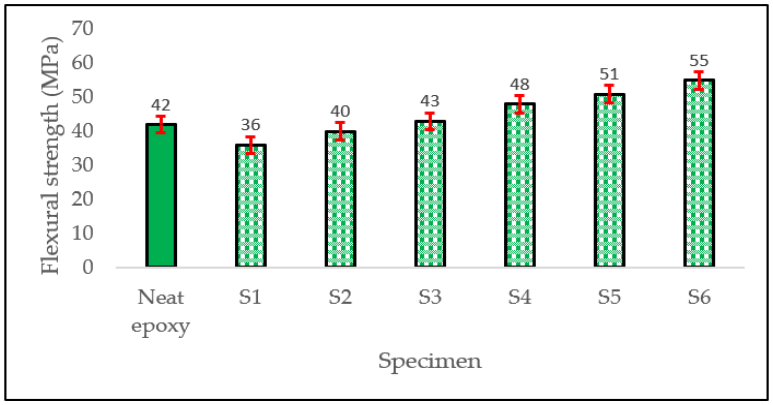

Figure 11. Flexural strength comparison of different compositions.

Representative flexural curves (Figure 12) show that fungal-treated composites (S6) sustain 15–20% higher strain before failure compared to untreated samples, attributed to mycelium networks delaying crack propagation. The post-peak stress drop is less severe in S6, suggesting enhanced energy absorption.

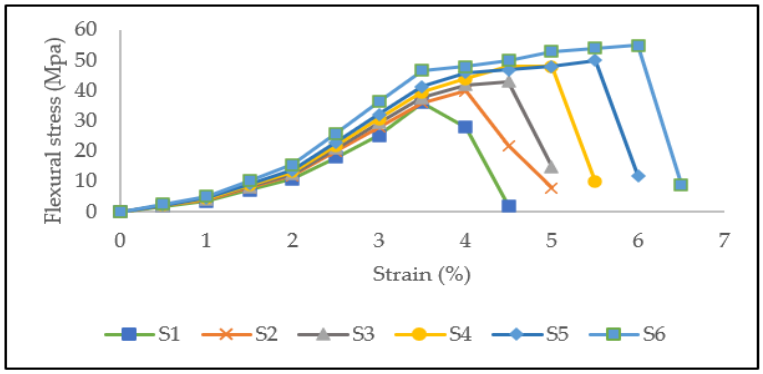

Figure 12. Representative flexural stress–strain curves.

Figure 13 illustrates the progressive improvement in impact strength with treatment. The untreated specimen (S1) exhibited an impact strength of 5.0 ± 2.5 kJ/m^2, representing the baseline toughness of the composite without any fiber treatment. Alkali-treated specimens (S2 and S3) showed improved impact strength values, ranging from 6.1 ± 3 kJ/m^2 to 7.0 ± 2.8 kJ/m^2, indicating that alkali treatment enhances the composite's ability to absorb energy under impact loading. The fungal-treated specimens (S4, S5, and S6) demonstrated further improvements, with impact strength values reaching 7.2 ± 2.3 kJ/m^2 to 8.6 ± 2.8 kJ/m^2. The highest impact strength was observed in specimen S6, which contained 25% sisal fiber and underwent both alkali and fungal treatments, achieving a value of 8.6 ± 2.8 kJ/m^2. Impact strength data were subjected to one-way ANOVA, revealing a statistically significant difference between groups (F = 4.24, p = 0.0049). This supports the conclusion that the treatments influenced the impact resistance of the composites.

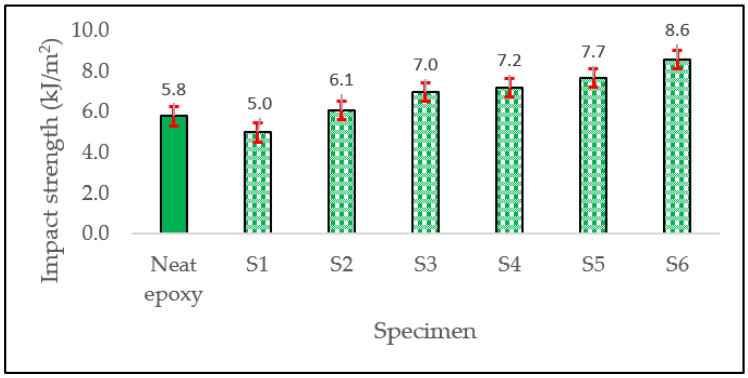

Figure 13. Impact strength comparison of different compositions.

Figure 14 highlights the shore hardness of the samples. The untreated specimen (S1) exhibited a Shore D hardness of 75 ± 5, representing the baseline surface hardness of the composite without any fiber treatment. Alkali-treated specimens (S2 and S3) showed a slight decrease in hardness, with values ranging from 72 ± 7 to 70 ± 5, suggesting that alkali treatment may slightly soften the composite surface due to fiber modification. In contrast, fungal-treated specimens (S4, S5, and S6) displayed a more noticeable reduction in hardness, with values ranging from 69 ± 6 to 68 ± 3. The lowest hardness value was observed in specimen S6, which contained 25% sisal fiber and underwent both alkali and fungal treatments, recording a hardness of 68 ± 3. These trends indicate that, while fungal treatment enhances mechanical properties, it may reduce surface hardness due to the formation of mycelium networks. Statistical analysis using one-way ANOVA yielded an F-value of 5.23 and a *p*-value of 0.0014 for Shore D hardness. This result confirms that the changes in surface hardness across treated and untreated samples are statistically significant.

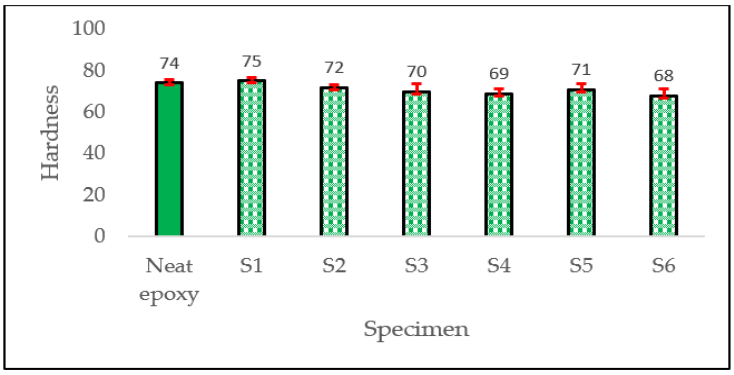

Figure 14. Shore D hardness comparison of different compositions.

3.2. Hydrophillic Properties

Figure 15 illustrates water absorption (%) of the samples. The untreated specimen (S1) exhibited significant water absorption, with the highest uptake observed over a 240 h immersion period. Alkali-treated specimens (S2 and S3) showed a moderate reduction in water absorption, indicating that alkali treatment reduces the hydrophilicity of the fibers by removing hemicellulose and lignin. Fungal-treated specimens (S4, S5, and S6) demonstrated further improvements, with the lowest water absorption values recorded. Specimen S6, which combined 25% sisal fiber and underwent both alkali and fungal treatments, exhibited the most resistance to water absorption, suggesting that fungal treatment enhances the composite's ability to repel moisture. However, even in the best-performing sample (S6), the water absorption remained significantly higher than that of neat epoxy, which was independently measured as 1.5% after 10 days of immersion. This indicates that the natural

fibers remain the primary contributors to moisture uptake in the composite system, despite surface treatments.

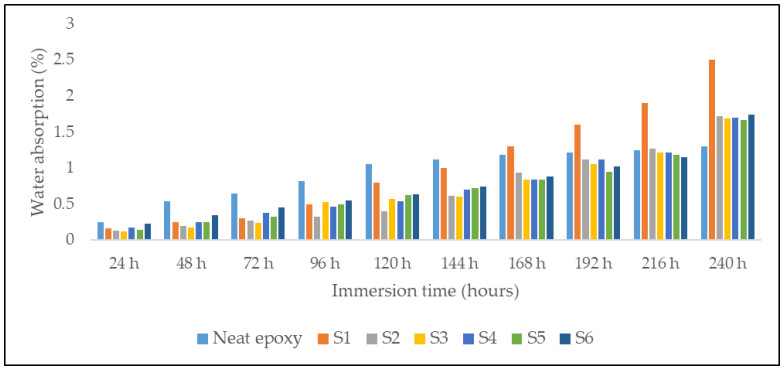

Figure 15. Water absorption comparison of different compositions.

To quantify the water diffusion behavior, the absorption data were fitted using Fick's second law for one-dimensional diffusion in a planar sheet. The initial portion of the absorption curves (up to 120 h) was used to extract diffusion coefficients based on the early-time approximation:

$$M_t = 4M_\infty \left(\frac{Dt}{\pi h^2} \right)^{\frac{1}{2}} \quad (5)$$

where M_t is the water absorption at time t, M_∞ is the equilibrium absorption at 240 h, and h is half the thickness (2 mm). Linear regression of M_t vs. $\sqrt{t}$ yielded the diffusion coefficient D for each formulation. The results are summarized in Table 6.

Table 6. Estimated diffusion coefficients from Fickian fit.

Specimen	Water Absorption at 240 h (%)	Diffusion Coefficient (m^2/s)
Neat epoxy	1.3	1.66×10^{-12}
S1	2.4	3.56×10^{-13}
S2	1.7	3.63×10^{-13}
S3	1.6	4.54×10^{-13}
S4	1.65	4.44×10^{-13}
S5	1.6	4.88×10^{-13}
S6	1.7	5.26×10^{-13}

3.3. Morphology Studies

The microstructure of the hemp and sisal fiber-reinforced hybrid composites was analyzed using optical microscopy.

Figure 16 reveals the microstructure of the untreated composite (S1), exhibiting improper resin filling areas and significant voids due to weak fiber–matrix adhesion. The lack of surface treatment resulted in poor wetting of hemp/sisal fibers by the epoxy matrix.

Figure 16. Optical microscopy of specimen S1 at 100 µm.

3.3.1. Alkali-Treated Specimens

Figure 17 highlights the microstructure of alkali-treated specimens. The images demonstrate improved fiber–matrix bonding compared to untreated specimens, with fewer voids and gaps. The removal of hemicellulose and lignin through alkali treatment results in a cleaner fiber surface, which enhances adhesion and contributes to the improved mechanical properties observed in these specimens.

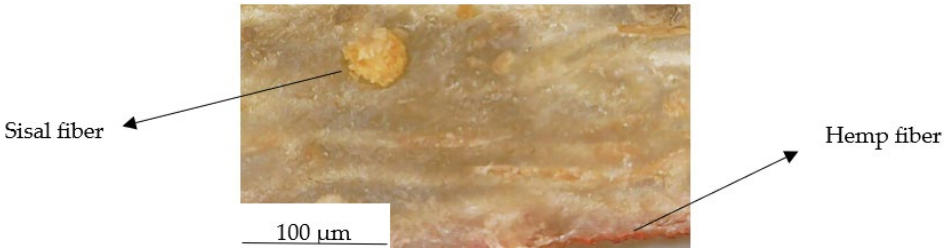

Figure 17. Optical microscopy image of alkali-treated specimen at 100 µm.

3.3.2. Fungal-Treated Specimens

Figure 18 displays the microstructure of fungal-treated specimens, showing the presence of mycelium networks on the fiber surfaces. This network creates a more uniform interface between the fibers and the matrix, further enhancing adhesion and mechanical performance. However, Figure 19 also reveals instances of mycelium breakage, which created micro-voids in some regions. These voids may explain the slight reduction in hardness observed in fungal-treated specimens.

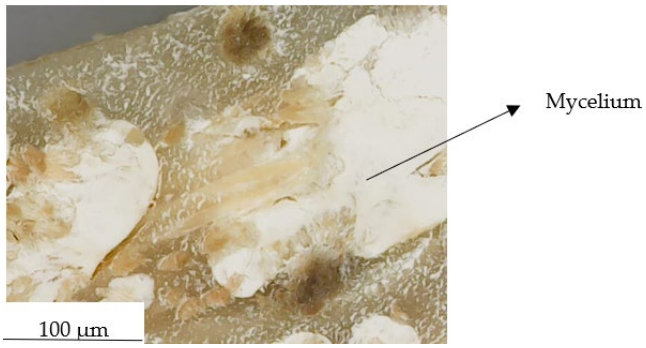

Figure 18. Optical microscopy image of mycelium networks on fiber surfaces at 100 µm.

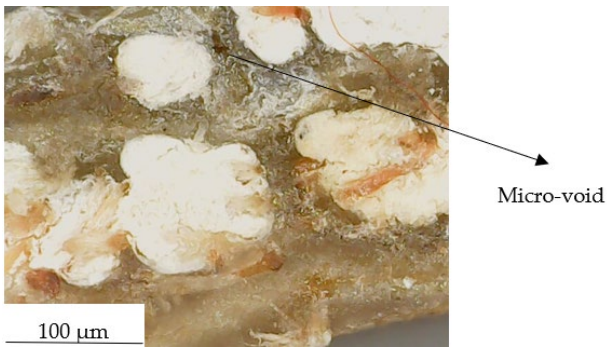

Figure 19. Optical microscopy image of mycelium breakage creating micro-voids at 100 µm.

3.3.3. Failure Analysis

Figures 20 and 21 present microscopy images of tensile-tested and impact-tested samples, respectively. In the tensile-tested sample (Figure 20), fibers are seen pulled in the

direction of loading, indicating effective stress transfer through the fiber–matrix interface. In impact-tested samples (Figure 21), the images show fibers pulling out and the matrix cracking, which are typical failure modes for fiber-reinforced composites under impact loading. These observations align with the mechanical performance data, confirming that treated specimens exhibit better resistance to failure due to improved interfacial bonding.

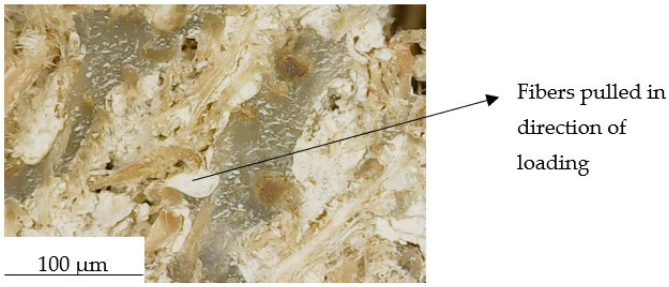

Figure 20. Optical microscopy of tensile-tested specimen at 100 μm.

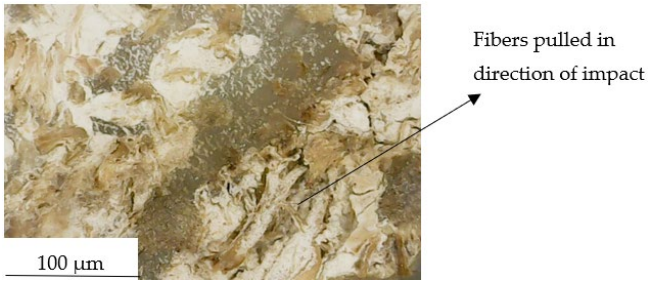

Figure 21. Optical microscopy of impact-tested specimen at 100 μm.

4. Discussion

The results of this study highlight the significant potential of alkali and fungal treatments in enhancing the mechanical and physical properties of hemp and sisal fiber-reinforced composites. The improvements observed in tensile, flexural, and impact properties, along with reduced water absorption, underscore the importance of these treatments in developing high-performance, sustainable composite materials.

The tensile, flexural, and impact properties of the composites showed marked improvements with alkali and fungal treatments. The untreated specimen (S1) exhibited baseline mechanical properties, while alkali-treated specimens (S2 and S3) demonstrated moderate improvements due to the removal of surface impurities and hemicellulose, which enhanced fiber–matrix adhesion. Fungal-treated specimens (S4, S5, and S6) displayed the most significant enhancements, with the highest tensile modulus (3227 MPa), tensile strength (55 MPa), flexural strength (55 MPa), and the impact strength (8.6 kJ/m^2). The fabric used in this study is randomly oriented, which limits the effective properties, such as modulus, due to load distribution in multiple directions. As a result, the measured modulus is approximately one-third of what would be expected with unidirectional alignment. Based on the rule of mixtures, a quantitative estimate with an assumed fiber volume fraction of 25%, epoxy modulus of 3 GPa, and average hemp and sisal fiber modulus of 45 and 15 GPa, respectively, yields a predicted composite modulus of 3.22 GPa for randomly oriented fibers (orientation factor $\eta_0 = 0.33$). This closely matches the experimentally measured modulus of 3.23 GPa for the best-performing specimen (S6), reinforcing the validity of the observed linear trend between fiber content and composite stiffness. While greater stiffness could be achieved with aligned fibers, this study focused on demonstrating improvements in fiber–matrix interaction through surface treatments.

Water absorption is a critical factor in determining the suitability of composites for applications in humid or wet environments. The untreated specimen (S1) exhibited the highest water absorption over the 240 h immersion period, while alkali-treated specimens (S2 and S3) showed a moderate reduction, attributed to the removal of hydrophilic components such as hemicellulose and lignin. Fungal-treated specimens (S4, S5, and S6) demonstrated the lowest water absorption, with specimen S6 showing the most resistance to moisture. This reduction in hydrophilicity is attributed to the formation of mycelium networks on the fiber surfaces, which act as partial barriers to moisture penetration. However, even in the best-performing specimen (S6), the water absorption remained significantly higher than that of neat epoxy, which was measured at 1.5% under the same conditions. To provide a quantitative comparison of water absorption behavior, Fickian diffusion coefficients were extracted using an early-time fit of the water uptake data. The untreated composite (S1) showed the lowest diffusion coefficient among the composites, while fungal-treated specimens (S4–S6) exhibited slightly higher coefficients, possibly due to increased surface area and micro-void formation. However, all treated composites demonstrated significantly lower diffusion coefficients than neat epoxy, confirming the barrier effect imparted by natural fibers and the treatments. This highlights that, despite surface treatments, the natural fibers continue to be the dominant contributors to water uptake. These findings suggest that, while surface modifications can improve moisture resistance, the composites may still face limitations in applications requiring high long-term durability in wet or humid conditions, such as automotive exteriors or structural components.

Optical microscopy provided valuable insights into the microstructure of the composites. Alkali-treated specimens showed improved fiber–matrix bonding with fewer voids and gaps, while fungal-treated specimens displayed mycelium networks that further enhanced adhesion. However, some micro-voids were observed in fungal-treated specimens, which may explain the slight reduction in hardness. The microscopy images also revealed effective stress transfer in tensile-tested specimens and typical failure modes (fiber pull-out and matrix cracking) in impact-tested specimens, confirming the improved mechanical performance of treated composites.

However, despite the improvements relative to untreated specimens, it is important to critically evaluate the limitations. While fungal and alkali treatments improved fiber–matrix bonding, the absolute mechanical properties and water resistance of the composites remain below those of conventional synthetic fiber composites such as glass fiber/epoxy systems. For example, glass fiber-reinforced epoxy composites typically show tensile strengths exceeding 300 MPa and water absorption below 0.3% after long-term immersion. In contrast, even the best-performing fungal-treated hybrid composites in this study achieved a maximum tensile strength of 55 MPa and exhibited significantly higher water uptake. This suggests that, although the treatments are effective relative to untreated natural fibers, the composites are not yet competitive for high-durability or structural applications.

Although this study utilized a conventional epoxy matrix, recent developments in bio-based resins offer promising alternatives that could enhance the overall sustainability of natural fiber composites. For example, Samper et al. [38] demonstrated that epoxidized linseed oil-based resins crosslinked with anhydrides provide comparable mechanical performance to petroleum-based epoxies. Similarly, Hasan et al. [39] highlighted the environmental advantages of using bio-resins in energy sector composites, indicating reduced carbon footprints and end-of-life impacts. Integrating such bio-resins with treated natural fibers could enable fully biodegradable composite systems in future work.

Overall, the treated natural fiber composites developed here show promise for low-load, non-structural applications such as packaging materials, interior panels, and construction components where moderate mechanical performance and moisture resistance

are acceptable. Their combination of renewability, partial biodegradability, and improved mechanical properties positions them as viable alternatives in sectors seeking greener material solutions, provided that the durability limitations are acknowledged.

5. Conclusions

This study demonstrates that alkali and fungal treatments significantly enhance the mechanical properties of hemp and sisal fiber-reinforced hybrid composites. Fungal treatment, in particular, offers a sustainable and effective method for improving fiber–matrix adhesion, resulting in composites with superior tensile, flexural, and impact properties compared to untreated counterparts. The treatments also contributed to reduced water absorption relative to untreated samples, although the absolute moisture uptake remains high compared to synthetic fiber composites. A Fickian analysis of water absorption further validated the moisture resistance improvement from treatments, showing diffusion coefficients 3–5 times lower than neat epoxy.

It is important to recognize that the use of biodegradable fibers partially improves the environmental profile of the composites, but the non-degradable epoxy matrix limits the overall sustainability at end-of-life. Therefore, while these composites contribute to the advancement of lightweight, renewable, and environmentally responsible materials, they are most suited for low-to-medium durability applications where biodegradability and moderate mechanical performance are prioritized over long-term stability.

6. Future Work

While this study demonstrates the potential of alkali and fungal treatments to enhance natural fiber composites, several important areas for future research remain. First, the optimization of fungal treatment conditions, including incubation time, substrate composition, and environmental parameters, is necessary to minimize the formation of micro-voids and further improve mechanical integrity. Second, given that the current epoxy matrix remains non-biodegradable, future work should prioritize the development of fully bio-based or biodegradable resin systems to achieve composites that are sustainable throughout their entire lifecycle. Finally, exploring a broader range of natural fibers and hybrid fiber architectures could expand the application potential of sustainable composites across industries requiring moderate mechanical performance and environmental responsibility.

Author Contributions: R.K. contributed to the data collection, synthesis, and writing of the initial drafts of the manuscript. J.S. helped with research progress and reviewing the report. R.K. developed the approach to the methodology. All authors have read and agreed to the published version of the manuscript.

Funding: This research received no external funding, and the APC was funded by Hochschule Kaiserslautern.

Data Availability Statement: The original contributions presented in this study are included in the article. Further inquiries can be directed to the corresponding author.

Acknowledgments: The Institute for Plastics Engineering West Pfalz (IKW) is acknowledged by the authors for its financial assistance. It is a research and testing facility run by the Department of Applied Logistics and Polymer Sciences at Hochschule Kaiserslautern, Pirmasens, Germany.

Conflicts of Interest: The authors declare no conflicts of interest.

References

1. Faruk, O.; Bledzki, A.K.; Fink, H.P.; Sain, M. Biocomposites reinforced with natural fibers: 2000–2010. *Prog. Polym. Sci.* **2012**, *37*, 1552–1596. [CrossRef]
2. Drzal, L.T. *Natural Fibers, Biopolymers, and Biocomposites*; CRC Press: Boca Raton, FL, USA, 2005.

3. Balaga, U.K.; Gunes, A.; Ozdemir, T.; Blackwell, C.; Davis, M.; Sauerbrunn, S.; Fuessel, L.; Deitzel, J.M.; Heider, D. Optimization of the Recycling Process for Aligned Short Carbon Fiber TuFF Composites. *Recycling* **2025**, *10*, 55. [CrossRef]
4. Pickering, K.L.; Efendy, M.A.; Le, T.M. A review of recent developments in natural fibre composites and their mechanical performance. *Compos. Part A Appl. Sci. Manuf.* **2016**, *83*, 98–112. [CrossRef]
5. Shahzad, A. Hemp fiber and its composites—A review. *J. Compos. Mater.* **2012**, *46*, 973–986. [CrossRef]
6. Bledzki, A.K.; Gassan, J. Composites reinforced with cellulose based fibres. *Prog. Polym. Sci.* **1999**, *24*, 221–274. [CrossRef]
7. Sathishkumar, T.P.; Naveen, J.A.; Satheeshkumar, S. Hybrid fiber reinforced polymer composites—A review. *J. Reinf. Plast. Compos.* **2014**, *33*, 454–471. [CrossRef]
8. Yan, L.; Chouw, N.; Jayaraman, K. Flax fibre and its composites—A review. *Compos. Part B Eng.* **2014**, *56*, 296–317. [CrossRef]
9. Baley, C. Analysis of the flax fibres tensile behaviour and analysis of the tensile stiffness increase. *Compos. Part A Appl. Sci. Manuf.* **2002**, *33*, 939–948. [CrossRef]
10. Saheb, D.N.; Jog, J.P. Natural fiber polymer composites: A review. *Adv. Polym. Technol. J. Polym. Process. Inst.* **1999**, *18*, 351–363. [CrossRef]
11. Thomason, J.L. The influence of fibre length and concentration on the properties of glass fibre reinforced polypropylene: 5. Injection moulded long and short fibre PP. *Compos. Part A Appl. Sci. Manuf.* **2002**, *33*, 1641–1652. [CrossRef]
12. Chawla, K.K.; Chawla, K.K. Carbon fiber composites. In *Composite Materials: Science and Engineering*; Springer: Cham, Switzerland, 1998; pp. 252–277.
13. Kumar, P.; Sharan Gupta, H.; Singh, M.; Chaudhari, A.S.; Maurya, A.K.; Manik, G. Mechanical, Thermal, and Morphological Analysis of Himalayan Agave Fiber/GO Coated Fly Ash Hybrid Polypropylene Composites. *Chem.–Eur. J.* **2025**, *31*, e202402393. [CrossRef] [PubMed]
14. John, M.J.; Anandjiwala, R.D. Recent developments in chemical modification and characterization oatural fiber-reinforced composites. *Polym. Compos.* **2008**, *29*, 187–207. [CrossRef]
15. Reddy, K.O.; Guduri, B.R.; Rajulu, A.V. Structural characterization and tensile properties of borassus fruit fibers. *J. Appl. Polym. Sci.* **2009**, *114*, 603–611. [CrossRef]
16. Reddy, K.O.; Reddy, K.R.N.; Zhang, J.; Zhang, J.; Varada Rajulu, A. Effect of alkali treatment on the properties of century fiber. *J. Nat. Fibers* **2013**, *10*, 282–296. [CrossRef]
17. Kommula, V.P.; Reddy, K.O.; Shukla, M.; Marwala, T.; Rajulu, A.V. Mechanical properties, water absorption, and chemical resistance of Napier grass fiber strand–reinforced epoxy resin composites. *Int. J. Polym. Anal. Charact.* **2014**, *19*, 693–708. [CrossRef]
18. Marquard, H.; Deshpande, A.M.; Aditya, S. Effect of Environmental Aging on the Thermal and Chemical Properties of Flax Fiber-Polypropylene Natural Fiber Reinforced Thermoplastic Composites. In Proceedings of the 2024 ASC Technical Conference, San Diego, CA, USA, 23–24 October 2024.
19. Sreekala, M.S.; Kumaran, M.G.; Thomas, S. Oil palm fibers: Morphology, chemical composition, surface modification, and mechanical properties. *J. Appl. Polym. Sci.* **1997**, *66*, 821–835. [CrossRef]
20. Gulati, D.; Sain, M. Fungal-modification of natural fibers: A novel method of treating natural fibers for composite reinforcement. *J. Polym. Environ.* **2006**, *14*, 347–352. [CrossRef]
21. Sałasińska, K.; Cabulis, P.; Kirpluks, M.; Kovalovs, A.; Kozikowski, P.; Barczewski, M.; Celiński, M.; Mizera, K.; Gałecka, M.; Skukis, E.; et al. The effect of manufacture process on mechanical properties and burning behavior of epoxy-based hybrid composites. *Materials* **2022**, *15*, 301. [CrossRef]
22. Bangaru, P.D.; Schuster, J.; Shaik, Y.P.; Müller, D. Evaluation of mechanical properties and hydrophilicity of alkaline and plasma treated abaca fiber epoxy composite with mineral waste as fillers. *J. Mater. Sci. Technol. Res.* **2024**, *11*, 15–24. [CrossRef]
23. Carl ROTH—International | Homepage. (n.d.). Available online: https://carlroth.com/ (accessed on 15 April 2024).
24. Kabir, M.M.; Wang, H.; Lau, K.T.; Cardona, F. Chemical treatments on plant-based natural fibre reinforced polymer composites: An overview. *Compos. Part B Eng.* **2012**, *43*, 2883–2892. [CrossRef]
25. Li, X.; Tabil, L.G.; Panigrahi, S. Chemical treatments of natural fiber for use in natural fiber-reinforced composites: A review. *J. Polym. Environ.* **2007**, *15*, 25–33. [CrossRef]
26. Zervakis, G.; Philippoussis, A.; Ioannidou, S.; Diamantopoulou, P. Mycelium growth kinetics and optimal temperature conditions for the cultivation of edible mushroom species on lignocellulosic substrates. *Folia Microbiol.* **2001**, *46*, 231–234. [CrossRef] [PubMed]
27. Gougouli, M.; Koutsoumanis, K.P. Relation between germination and mycelium growth of individual fungal spores. *Int. J. Food Microbiol.* **2013**, *161*, 231–239. [CrossRef]
28. Schuster, J.; Govignon, Q.; Bickerton, S. Processability of biobased thermoset resins and flax fibres reinforcements using vacuum assisted resin transfer moulding. *Open J. Compos. Mater.* **2014**, *4*, 1–11. [CrossRef]
29. Bender, D.; Schuster, J.; Heider, D. Flow rate control during vacuum-assisted resin transfer molding (VARTM) processing. *Compos. Sci. Technol.* **2006**, *66*, 2265–2271. [CrossRef]

30. Abdurohman, K.; Satrio, T.; Muzayadah, N.L.; Teten. A comparison process between hand lay-up, vacuum infusion and vacuum bagging method toward E-glass EW 185/lycal composites. *J. Phys. Conf. Ser.* **2018**, *1130*, 012018. [CrossRef]
31. Mujahid, Y.; Sallih, N.; Abdullah, M.Z.; Mustapha, M. Effects of processing parameters for vacuum-bag-only method on void content and mechanical properties of laminated composites. *Polym. Compos.* **2021**, *42*, 567–582. [CrossRef]
32. Hall, W.; Javanbakht, Z.; Hall, W.; Javanbakht, Z. Advanced methods—Vacuum bagging and prepreg moulding. In *Design and Manufacture of Fibre-Reinforced Composites*; Springer: Cham, Switzerland, 2021; pp. 55–68.
33. EN ISO 527-5:2009; Plastics–Determination of Tensile Properties. *British Standard*; BSEN ISO: London, UK, 1997.
34. *DIN EN ISO 178*; Plastics—Determination of Flexural Properties. International Organization for Standardization: Geneva, Switzerland, 2019.
35. *DIN EN ISO 179*; Plastics—Determination of Charpy impact properties. International Organization for Standardization: Geneva, Switzerland, 2010.
36. *DIN 53505*; Testing of rubber—Determination of hardness (Shore Hardness). Deutsches Institut für Normung: Berlin, Germany, 2000.
37. *ASTM D570-98*; Standard Test Method for Water Absorption of Plastics. ASTM International: West Conshohocken, PA, USA, 1998.
38. Samper, M.D.; Ferri, J.M.; Carbonell-Verdu, A.; Balart, R.; Fenollar, O. Properties of biobased epoxy resins from epoxidized linseed oil (ELO) crosslinked with a mixture of cyclic anhydride and maleinized linseed oil. *Express Polym. Lett.* **2019**, *13*, 407–418. [CrossRef]
39. Hasan, M.Z.; Salit, M.S.; Hamdan, N.S.; Aziz, F.A.; Khan, A. Environmental life cycle analysis of natural fiber composites in energy sector. *Phys. Sci. Rev.* **2025**, *10*, 229–243. [CrossRef]